Turkish Journal of Electrical Engineering and Computer Sciences

Volume 25 | Number 5 Article 42

1-1-2017

Design of a sharp response microstrip lowpass filter using taper loaded and radial stub resonators

SOHRAB MAJIDIFAR

MOHSEN HAYATI

Turkish Journal of Electrical Engineering & Computer Sciences

http://journals.tubitak.gov.tr/elektrik/

Research Article

Turk J Elec Eng & Comp Sci
(2017) 25: 4013 – 4022

doi:10.3906/elk-1609-130

Design of a sharp response microstrip lowpass filter using taper loaded and radial stub resonators

Sohrab MAJIDIFAR[1,*], **Mohsen HAYATI**[2]

[1]Department of Electrical Engineering, Kermanshah University of Technology, Kermanshah, Iran
[2]Department of Electrical Engineering, Kermanshah Branch, Islamic Azad University, Kermanshah, Iran

Received: 14.09.2016 • **Accepted/Published Online:** 17.02.2017 • **Final Version:** 05.10.2017

Abstract: This paper proposes a compact microstrip lowpass filter with a wide stopband and a very sharp roll-off. This structure consists of two dual taper-loaded resonators that are connected to the radial stubs. The resonators are described using an LC model, and its Z- and S-parameters are extracted as a function of the LC component. In the proposed filter, cut-off frequency is placed at 1.76 GHz, roll-off rate is higher than 142 dB/GHz, insertion loss is less than 0.42 dB from DC to 1.5 GHz, and rejection is greater than –24 dB from 1.88 to 15.2 GHz. The proposed filter is designed, fabricated, and measured, and the measured values are in good agreement with the EM-simulated results.

Key words: Lowpass filter, circuit model, scaling, EM simulation

1. Introduction

Microstrip lowpass filters (LPFs) with compact size and high performance are widely applied in communication systems for suppression of unwanted signals. These filters appear in various shapes. Nevertheless, in the designing process of the novel structures, the main purpose is to improve the response parameters such as stopband bandwidth, selectivity, and compactness. Researchers have used different methods to realize these goals. Several articles have focused on sharpness improvement [1–3]. In [1], a compact LPF with high selectivity is obtained by combining three shunt open stubs. A compact structure with high selectivity was designed in [2], which is composed of two folded stepped impedance open stubs. In [4–8], researchers designed LPFs with a wide stopband. In [4], a novel meandered-slot resonator was presented to design an LPF with a wide stopband. This LPF reaches an ultrawide stopband of 12.8 times the cut-off frequency and with attenuation higher than 20 dB. A bandstop structure has been embedded into a classical stepped impedance LPF in [7] to increase the width of the stopband. This filter has a small size. A high-performance LPF with a compact size, wide stopband, and sharp rejection has been proposed in [9]. In [10], a symmetrical coupled line has been proposed to design a wide stopband LPF. The authors in [11–14] focus on compactness in LPF design.

In this paper, we propose a new structure for the design of an LPF with very sharp rejection, wide stopband, and compact size. Initially, the proposed dual taper-loaded resonator is presented and studied, and then it is used to implement a high-performance LPF. The resonators are described using the LC model, and their Z- and S-parameters are extracted as a function of the LC component. In the proposed filter, the cut-off frequency is placed at 1.76 GHz, the roll-off rate is higher than 142 dB/GHz, and the circuit size is 0.215 $\lambda_g \times$

*Correspondence: sohrab.majidi@gmail.com

0.1 λ_g. This LPF achieves a wide stopband with an overall 24-dB attenuation up to 7.56 times the 3-dB cut-off frequency.

2. Proposed structure

The layout of the proposed structure is shown in Figure 1a. In this resonator, two taper-loaded cells are connected with a central simultaneity point. This resonator creates two near-band attenuation zeros that result in a sharp roll-off and a deep rejection in the low-frequency region of the stopband. The dimensions in Figure 1a are: l1 = 7.75 mm, l2 = 6.3 mm, l3 = 6.1 mm, l4 = 0.95 mm, l5 = 3.55 mm, l6 = 5.2 mm, w1 = 0.2 mm, w2 = 0.2 mm, w3 = 0.1 mm, w4 = 1.83 mm, and h = 4.6 mm. This resonator is designed on an RT/Duroid 5880 substrate with 2.2 dielectric constant, 15 mil height, and 0.0009 loss tangent. Figure 1b shows the approximate equivalent LC circuit of the proposed resonator. The parts of this circuit are introduced and then the behavior of the resonator is studied.

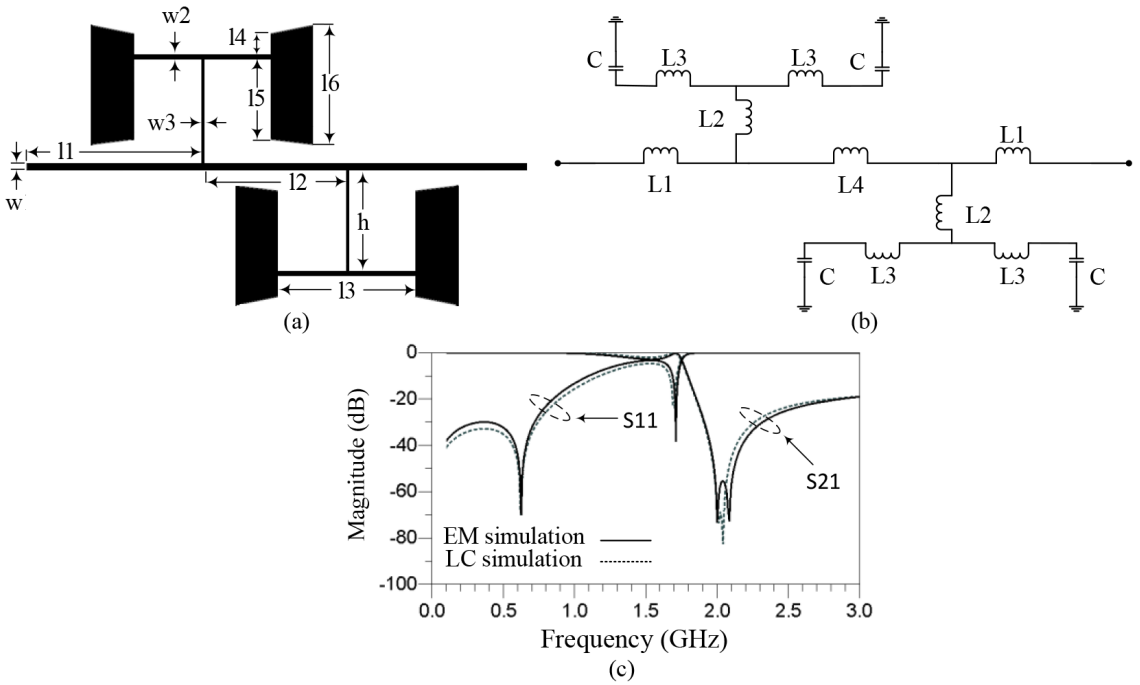

Figure 1. Proposed resonator: a) layout, b) equivalent LC circuit, c) EM and LC simulation.

L1 and L4 are inductances of the central transmission line. The inductances of the T-shaped line are introduced by L2 and L3. C shows the body capacitance of the tapered shape.

The calculated characteristic impedance (Z_c) and effective permittivity (ε_{re}) are Z_c = 154 Ω and ε_{re} = 1.695 for w = 0.1, Z_c = 123 Ω and ε_{re} = 1.728 for w = 0.2, and ε_{re} = 1.94 and Z_c = 36.5 Ω for w = 1.83. The LC parameters are calculated as follows [2], [15–16]: L1 = 3.2 nH, L2 = 2.7 nH, L3 = 1.4 nH, L4 = 3.52 nH, and C = 0.84 pF.

The LC and EM simulated results of the resonator are shown in Figure 1c.

Figures 2 and 3 show two synthesis methods to adapt the proposed resonator to different specifications. The sharpness and the cut-off frequency of the LC resonator as a function of L1, L2, L3, L4, and C are shown in Figure 2.

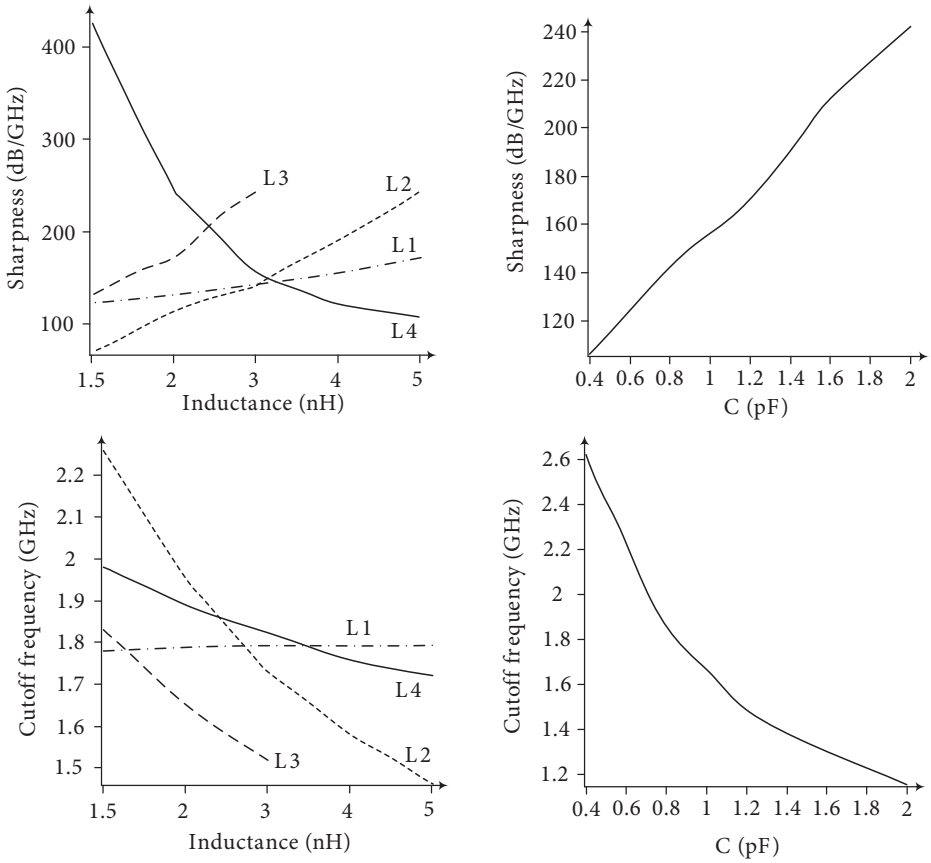

Figure 2. Sharpness and cut-off frequency of the LC resonator as a function of L1, L2, L3, L4, and C.

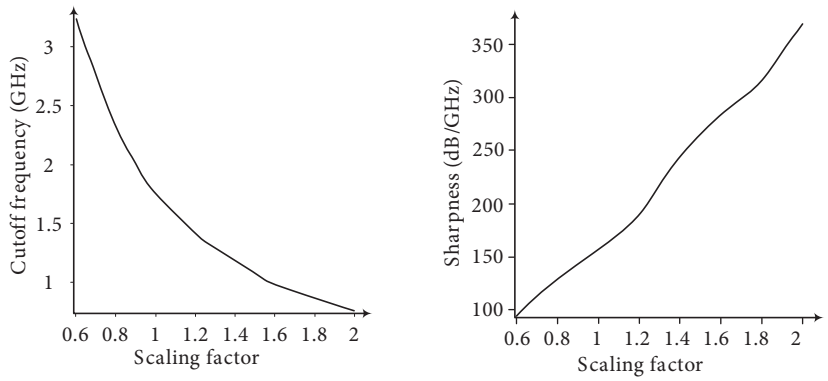

Figure 3. Sharpness and cut-off frequency of the resonator as a function of the scaling factor.

Another synthesis method is presented using resonator scaling. Figure 3 shows the sharpness and cut-off frequency of the resonator as a function of the scaling factor (scaling all the resonator dimensions with a constant factor).

The $Z_{21} = Z_{12}$ and $Z_{11} = Z_{22}$ of the proposed LC resonator are a function of L2, L3, L4, C, and f, as follows:

$$|Z_{21}| = |Z_{12}| = 0.125I(8\pi^2 f^2 CL2 + 4L3\pi^2 f^2 C - 1)^2/C\pi f(8L2\pi^2 f^2 C + 4\pi^2 f^2 CL3 + 4\pi^2 f^2 CL4 - 1) \quad (1)$$

$$|Z_{11}| = |Z_{22}| = 0.125I(1 + 64\pi^4 f^4 C^2 L2L4 + 32\pi^4 f^4 C^2 L3L4 - 8L4\pi^2 f^2 C + 64\pi^4 f^4 C^2 L2^2 + 64\pi^4 f^4 C^2 L2L3 - 16\pi^2 f^2 CL2 + 16\pi^4 f^4 C^2 L3^2 - 8\pi^2 f^2 CL3 + 128\pi^4 f^4 C^2 L2L1 + 64\pi^4 f^4 C^2 L1L3 - 16\pi^2 f^2 CL1 + 64\pi^4 f^4 C^2 L1L4)/ c\pi f(8L2\pi^2 f^2 C + 4\pi^2 f^2 CL3 + 4\pi^2 f^2 CL4 - 1) \quad (2)$$

$|S_{21}|$ of the LC resonator is as follows:

$$|S_{21}| = (12.5I(8\pi^2 f^2 CL2 + 4\pi^2 f^2 CL3 - 1)^2)/ (c\pi f(-1 + 8L2\pi^2 f^2 C + 4\pi^2 f^2 CL3 + 4\pi^2 f^2 CL4) (((0.125I(-1 + 8L2\pi^2 f^2 C + 4\pi^2 f^2 CL3) (-1 + 8L4\pi^2 f^2 C + 8\pi^2 f^2 CL2 + 4\pi^2 f^2 CL3)/ (c\pi f(-1 + 8L2\pi^2 f^2 C + 4\pi^2 f^2 CL3 + 4\pi^2 f^2 CL4)) +50)^2 + 0.0156(-1 + 8L2\pi^2 f^2 C + 4\pi^2 f^2 CL3)^4/ (c^2\pi^2 f^2(-1 + 8L2\pi^2 f^2 C + 4\pi^2 f^2 CL3 + 4\pi^2 f^2 CL4)^2))) \quad (3)$$

where f represents the frequency at Hz. If in Eq. (3) we set L1 = 3.2 nH, L2 = 2.7 nH, L3 = 1.4 nH, L4 = 3.52 nH, and C = 0.84 pF, then $|S_{21}|$ turns to a function of f as in Eq. (4):

$$|S_{21}| = (1.48810^{13} I(-1 + 2.28510^{-20}\pi^2 f^2)^2)/ (\pi f(-1 + 3.4710^{-20}\pi^2 f^2)((1/ (\pi f(-1 + 3.4710^{-20}\pi^2 f^2))(1.48810^{11} I (-1 + 2.28510^{-20}\pi^2 f^2)(-1 + 4.6510^{-20}\pi^2 f^2))+ 50)^2 + (2.2110^{22}(-1 + 2.28510^{-20}\pi^2 f^2)^4)/ (\pi^2 f^2(-1 + 3.4710^{-20}\pi^2 f^2)))) \quad (4)$$

To verify the validity of these equations, Figure 4 shows the magnitude of S_{21} as a function of f (according to Eq. (4)).

The sharpness of the resonator is introduced by Eq. (5):

$$\Delta f = f_s - f_c, \quad (5)$$

where f_s is the first –20 dB point and f_c is the 3dB cut-off frequency of the resonator. Let f_c be the smallest positive root of Eq. (6) and f_s denote the positive root of Eq. (7). Then Eq. (5) defines the sharpness of the LC resonator response.

$$A = 20\log|S_{21}(f)| + 3 = 0 \quad (6)$$

$$B = 20\log|S_{21}(f)| + 20 = 0 \quad (7)$$

Figure 5 depicts Δf in terms of C, L2, L3, and L4.

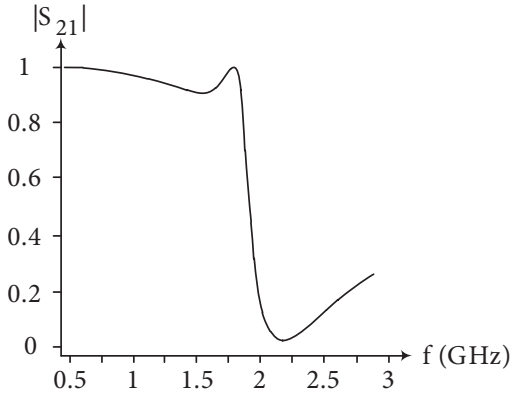

Figure 4. Magnitude of the S_{21} as a function of f, according to Eq. (4).

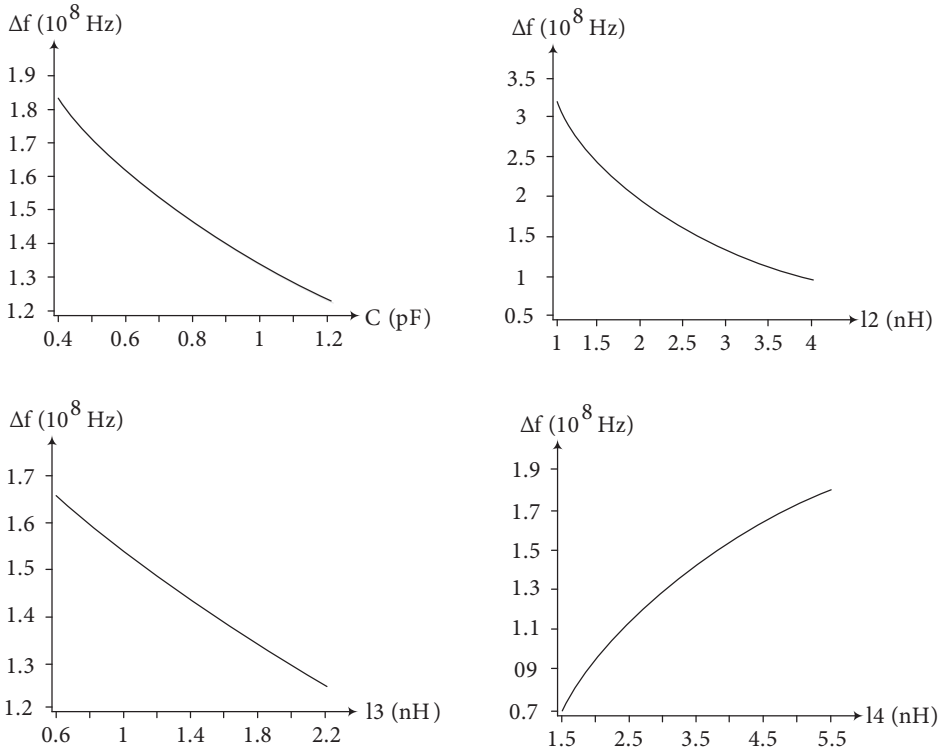

Figure 5. Sharpness of the LC resonator response as a function of C, L2, L3, and L4.

3. Filter design and results and discussion

Figure 1c shows the simulated response of the proposed resonator, which has a limited stopband and low rejection. To solve this problem, two patched radial stubs are cascaded with the resonator to form the proposed filter. Figure 6 shows the layout, equivalent LC model, and LC/EM simulation results of the radial stub resonator. In this model, the series-connected L_r and grounded C_r introduce the radial stub, and L_q represents the inductance of the central line. The dimensions of this structure are as follows: wi = 2 mm, l4 = 6.2 mm, r = 4.7 mm, and $\alpha = 54^\circ$.

Using Eqs. (8–11) and some optimization [2,15–16], these LC parameters are calculated as $L_r = 0.09$

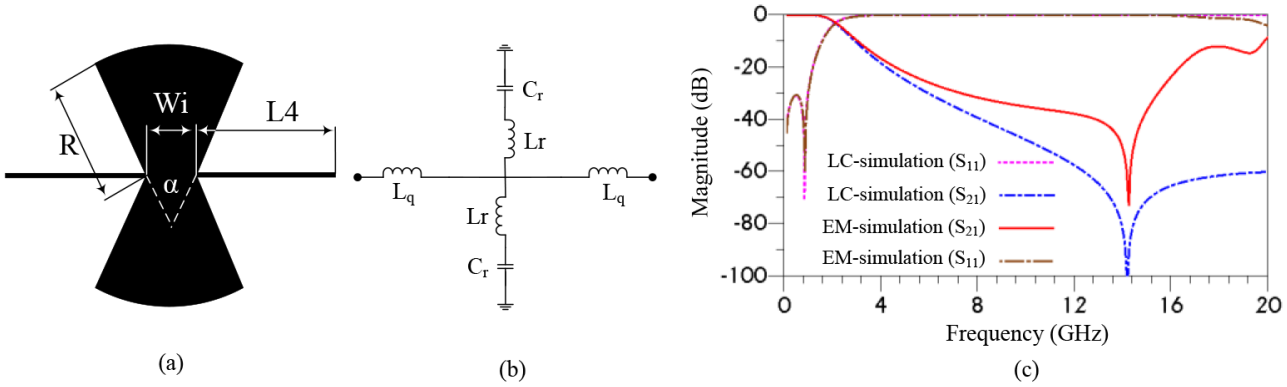

Figure 6. Radial stub resonator: a) layout, b) equivalent LC model, c) LC/EM simulation results.

nH, C_r = 1.4 pF, and L_q = 4.2 nH.

$$L = \frac{lz_c}{v_p} \tag{8}$$

$$v_p = \frac{c}{\sqrt{\varepsilon_{re}}} \tag{9}$$

For w/h $\leq$ 1

$$\varepsilon_{re} = \frac{\varepsilon_r + 1}{2} + \frac{\varepsilon_r - 1}{2}\{[1 + 12\frac{h}{w}]^{-0.5} + 0.04[1 - \frac{w}{h}]^2\},\ z_c = \frac{\eta}{2\pi\sqrt{\varepsilon_{re}}} \ln[8\frac{h}{w} + 0.25\frac{w}{h}] \tag{10}$$

For w/h $\geq$1

$$\varepsilon_{re} = \frac{\varepsilon_r + 1}{2} + \frac{\varepsilon_r - 1}{2}[1 + 12\frac{h}{w}]^{-0.5},\ z_c = \frac{\eta}{\sqrt{\varepsilon_{re}}}\{\frac{w}{h} + 1.393 + 0.677\ln[\frac{w}{h} + 1.444]\}^{-1} \tag{11}$$

Figure 7 shows the sharpness and cut-off frequency of the LC radial stub resonator as a function of L_r, C_r, and L_q.

Sharpness and cut-off frequency of the radial stub resonator as a function of the scaling factor are shown in Figure 8.

Δf_1 has been calculated using the S_{21} function of the radial stub resonator, similarly to the Δf for the LC radial stub resonator. Figure 9 shows the Δf_1 as a function of L_r, C_r, and L_q.

Figure 10 shows the layout, photograph, and simulation results of the proposed filter. The dimensions of the proposed filter are as follows:

w1 = 1.15 mm, wi = 2 mm, m1 = 2.5 mm, m2 = 3 mm, m3 = 7.7 mm, m4 = 6.2 mm, h1 = 4.6 mm, h2 = 4.87 mm, h3 = 4.55 mm, h4 = 4.6 mm, r = 4.7 mm, and $\alpha = 54°$.

The simulation was accomplished using an EM simulator (ADS), and measurements were performed using an Agilent network analyzer N5230A. As depicted in Figure 10c, the 3-dB cut-off frequency is placed at 1.76 GHz, and a stopband is reached from 1.88 to 15.2 GHz with a higher than 24 dB attenuation level. The insertion loss is less than 0.4 dB from DC to 1.5 GHz. The return loss is higher than 11 dB in the passband and is close to 0 dB in the stopband.

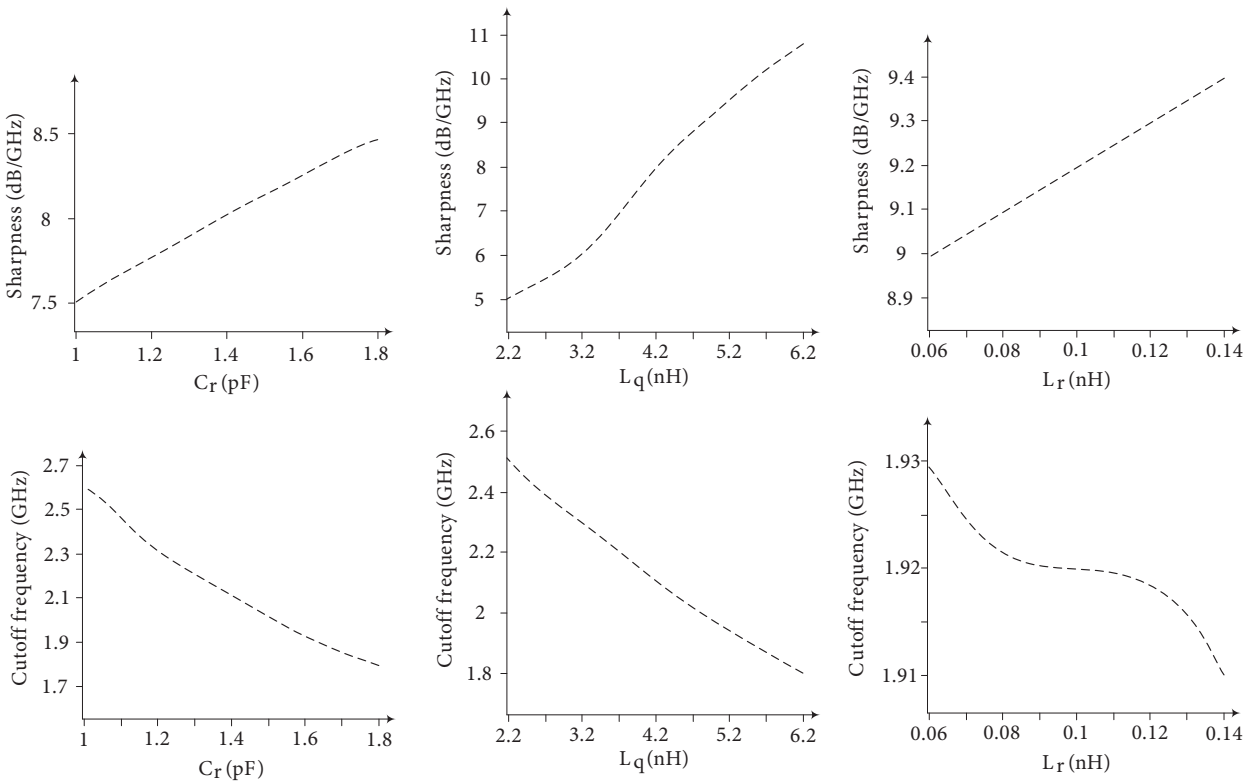

Figure 7. Sharpness and cut-off frequency of the LC radial stub resonator as a function of L_r, C_r, and L_q.

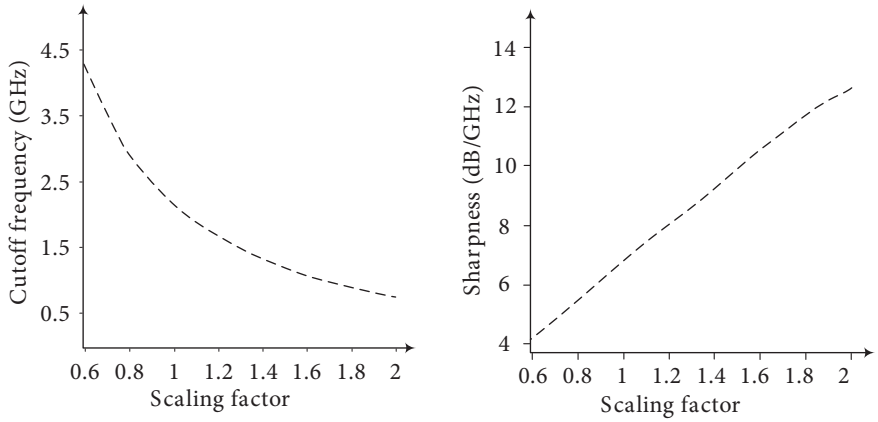

Figure 8. Sharpness and cut-off frequency of the radial stub resonator as a function of the scaling factor.

Table 1 compares the performance of the proposed filters in terms of stopband bandwidth, rejection level in the stopband, sharpness, physical size, and passband losses level with the previous works. This comparison is based on the equations and parameters of Table 2 [9,13]:

α_{max}, α_{min}, f_s, f_c and λ_g are introduced in Table 3.

As shown in Table 1, the response of the proposed filter is sharper than in [1,2,4,5,7–14], its stopband bandwidth is wider than in [1–3,5,7,8,10–14], its rejection level is better than in [1,2,4–8,10–14], and normalized circuit size of the proposed filter is better than in [1,2,4–7,10,11,14].

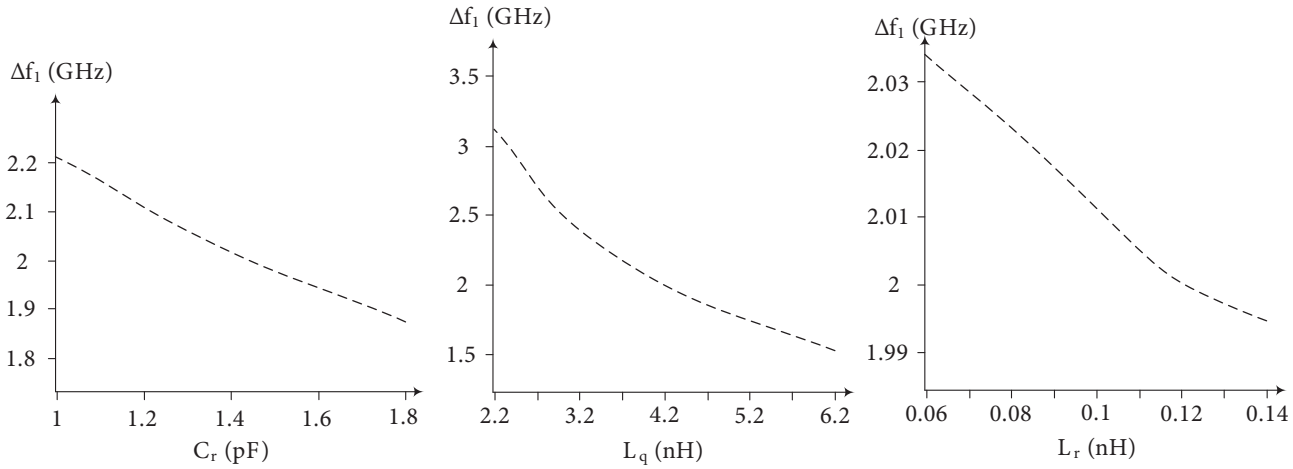

Figure 9. Δf_1 as a function of L_r, C_r, and L_q.

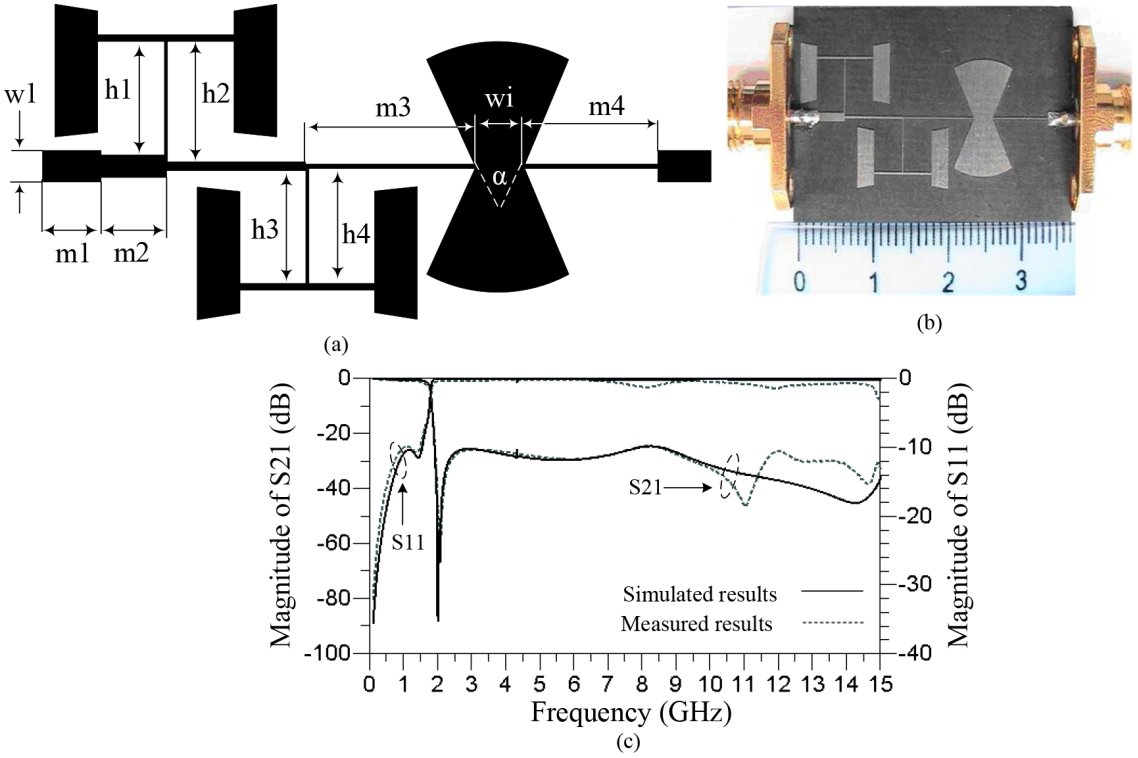

Figure 10. Proposed filter: a) layout, b) photograph, c) simulation and measurement results.

4. Conclusion

In this paper, a high-performance lowpass filter, based on taper loaded units, is designed, fabricated, and measured. The physical size of the filter is 0.215 $\lambda_g \times$ 0.1 λ_g. The measured results indicate a wide stopband of 13.32 GHz with an attenuation level higher than 24 dB and a very sharp transition band with a rate of 142 dB/GHz. Its compactness, sharp rejection, and wide stopband make this LPF suitable for microwave applications.

Table 1. Performance comparison among proposed filter and referenced works.

Article	fc (GHz)	SBW (GHz)	MA (dB)	ς (dB/GHz)	NCS	IL (dB)	RL (dB)
This work	1.76	13.32	24	142	0.0215	0.4	11
[1]	2.49	4.2	20	54.8	0.0323	0.26	22
[2]	2.28	12.47	20	121.4	0.0338	0.14	12.3
[3]	1.49	5.76	20	134.55	0.1495	0.85	13.5
[4]	2.2	28.16	20	58.6	0.055	0.5	10
[5]	1.76	12.32	20	51.5	0.048	0.6	8.5
[6]	1.8	29.7	20	250	0.251	0.3	-
[7]	1.8	5.04	16	34	0.031	0.5	10
[8]	2	10.3	20	24.29	0.0094	0.6	12
[9]	1.89	17.94	25	121.5	0.0177	0.5	10
[10]	0.8	6.42	16	68	-	0.1	27
[11]	2.2	5.28	23	85	0.051	< 0.5	13
[12]	1.3	12.22	17	21	0.0088	0.3	-
[13]	1.18	7	15	36.3	0.0062	-	> 20
[14]	3.09	15.17	20	45.95	0.031	0.5	10

Table 2. Basic parameters for comparing LPF responses.

Parameters	Symbol	Equation or definition
Stopband bandwidth (GHz)	SBW	Stopband bandwidth of the LPF response
Rejection level in stopband (dB)	MA	Max attenuation level in the stopband
Sharpness (dB/GHz)	ζ	$\zeta = \frac{a_{\max} - a_{\min}}{fs - fc}$
Normalized circuit size	NCS	$NCS = \frac{\text{physical size}}{\lambda g^2}$
Passband losses level (dB)	IL	Passband ripple level
	RL	Return loss in passband

Table 3. Description of the α_{max}, α_{min}, f_s, f_c, and λ_g.

Phrase	Description
α_{max}	3 dB attenuation point
α_{min}	20 dB attenuation point
f_s	20 dB stopband frequency
f_c	3 dB cut-off frequency
λ_g	Guided wavelength at 3 dB cut-off frequency

References

[1] Yang RY, Lin YL, Hung CY, Lin CC. Design of a compact and sharp rejection low-pass filter with a wide stopband. J Electromagnet Wave 2012; 26: 2284-2290.

[2] Makki SV, Ahmadi A, Majidifar S, Sariri H, Rahmani Z. Sharp response microstrip LPF using folded stepped impedance open stubs. Radio Eng 2013; 22: 328-332.

[3] Ertay AO, Abbak M, Simsek S. An improved stopband and sharp roll off microstrip low pass filter with defected ground structures. Int J Microw Wirel Technol 2016; 8: 573-581.

[4] Cao HL, Ying WB, Li H, Yang SZ. Compact lowpass filter with ultra-wide stopband rejection using meandered-slot dumbbell resonator. J Electromagnet Wave 2012; 26: 2203-2210.

[5] Cao H, Ying W, Li H, Yang S. Compact lowpass filter with wide stopband using novel windmill resonator. J Electromagnet Wave 2012; 26: 2234-2241.

[6] Taher H. Ultra wide stopband low-pass filter using triangular resonators defected ground. J Electromagnet Wave 2014; 28: 542-550.

[7] He Q, Liu C. A novel low-pass filter with an embedded band-stop structure for improved stop-band characteristics. IEEE Microw Wirel Co 2009; 19: 629-631.

[8] Yang MH, Xu J, Zhao Q, Peng L, Li GP. Compact, broad-stopband lowpass filters using SIRs-loaded circular hairpin resonators. Prog Electromagnet Res 2010; 102: 95-106.

[9] Karimi Gh, Siahkamari H, Khamin F, Lalbakhsh A. Design of modified Z-shaped and T-shaped microstrip filter based on transfer function analysis. Wireless Pers Comm 2015; 82: 2005-2016.

[10] Wu Y, Liu Y, Li S, Yu C. A new wide-stopband low-pass filter with generalized coupled-line circuit and analytical theory. Prog Electromagnet Res 2011; 116: 553-567.

[11] Fu SH, Ong CM, Li XM, Zhang W, Shen K. Compact miniaturized stepped impedance low-pass filter with sharp cut-off characteristic. Microw Opt Techn Let 2009; 51: 2257-2258.

[12] Ge L, Wang JP, Gue YX. Compact microstrip low-pass filter with ultra-wide stopband. Electron Lett 2009; 46: 689-691.

[13] Wang J, Xu LJ, Zhao S, Guo YX, Wu W. Compact quasi-elliptic microstrip lowpass filters with wide stopband. Electron Lett 2010; 46: 1384-1385.

[14] Sariri H, Rahmani Z, Lalbakhsh A, Majidifar S. Compact LPF using T-shaped resonator. Frequenz 2013; 67: 17-20.

[15] Che W, Tang YF, Zhang J, Chow YL. Formulas of dielectric and total attenuations of a microstrip line. Radio Sci 2010; 42.

[16] Hong JS, Lancaster MJ. Microstrip Filters for RF/Microwave Applications. New York, NY, USA: Wiley, 2001.